

# Rapid sintering and microstructure evolution of composite TiC cermet

L Ding<sup>1,2</sup>, X G Liu<sup>1,2</sup>, Y L Pan<sup>1,2</sup>, Y W Wang<sup>1,2</sup> and D P Xiang<sup>1,2,3</sup>

<sup>1</sup> State Key Laboratory of Marine Resource Utilization in South China Sea, Hainan University, Haikou 570228, China

<sup>2</sup> Key Laboratory of Advanced Materials of Tropical Island Resources, Ministry of Education, Hainan University, Haikou 570228, China

E-mail: dpxiang@hainu.edu.cn

**Abstract.** Ti, Ni, activated carbon, and Mo powders were used as raw materials to prepare a composite TiC cermet in this study. The powders were mixed and prepared through high-energy ball milling and then sintered in a spark plasma sintering (SPS) system. Results revealed that ball milling time affected the raw materials. After ball milling was performed for 10 h, Ti and C particles reacted and generated TiC, meanwhile, the solid Mo solutionized in TiC and formed (Ti,Mo)C lumps. XRD results showed that the product of (Ti,Mo)C cermet with high hardness can be prepared at a low sintering temperature of 1150 °C. The microstructure of composite TiC cermet was different from the traditional core-ring structure. In particular, the developed microstructure comprises a (Ti,Mo)C-Ni dark-gray phase at the center surrounded by (Ti,Mo)C light-gray phase and dispersed Mo white phase.

## 1. Introduction

TiC cermet is a metal matrix composite extensively investigated as a promising material for high-temperature structural applications because of its high melting point, hardness, and corrosion resistance [1-2]. Traditional TiC cermet preparation is relatively complex, and high sintering temperature and difficult control of both product purity and batch production significantly hinder the improvement of TiC properties [3-6]. As an advanced rapid sintering technique, spark plasma sintering (SPS) requires lower temperature and shorter time than other sintering techniques do [7-8]. In our study, high-energy ball milling (HEBM) and SPS technologies were examined and used to prepare composite TiC cermet. Ti, Ni, activated carbon, and Mo powders were used as raw materials, mixed through HEBM, and sintered in a SPS system to prepare the composite TiC cermet. The effects of HEBM time on the composite powders were investigated. Meanwhile, the effects of sintering temperature on the microstructural evolution of composite TiC cermet were also determined.

## 2. Experimental

The raw materials used in this study were Ti, Ni, activated carbon, and Mo powders (>99.5 wt.% purity). The average particle size was approximately 3.0 μm for Ti powder, 2.8 μm for activated carbon, and 1 μm for Ni and Mo powders. The powders were mixed, and prepared by high-energy ball milling with Ar protection. The ball-to-powder weight ratio was set to 10:1, and WC-cemented carbide balls were used as grinding media. The ball milling speed was 580 rpm for 10h of milling time. Subsequently, powder mixture was retrieved, filled in vacuum glove box mould, and eventually



sintered in SPS. The sintering equipment utilized in the experiment was the SPS LABOXTM-3010K sintering system. The powders were sintered in the SPS system for 5 min at a pressure of 20 MPa, a temperature of 1150 °C to 1450 °C, and a heating rate of 100 °C/min by sintering. The samples were cooled to room temperature and removed from the furnace. Hardness was measured by the digital HRS-150 Rockwell hardness tester. All of the samples were subjected to X-ray diffraction (XRD) for phase composition analysis. Scanning electron microscopy (SEM) with a S-4800 Type II microscope was used to observe the microstructure of the sintered samples.

### 3. Results and discussion

#### 3.1. Effects of mechanical ball milling time on the raw powders

Figure 1 shows the external view of the raw materials at different ball milling times. After different milling times of 5 and 10 h, the color and state of the raw materials varied. After ball milling was conducted for 5 h, the powders with a small particle size were dark gray. The mixture was very uniform, and the powder was very fine. After ball milling was performed for 10 h, the materials formed large lumps with varying sizes. The gray lumps contained apparent pores and exhibited a high hardness value. After measurement was conducted, the hardness of the raw material ball-milled for 10 h was 82.6 HRA.

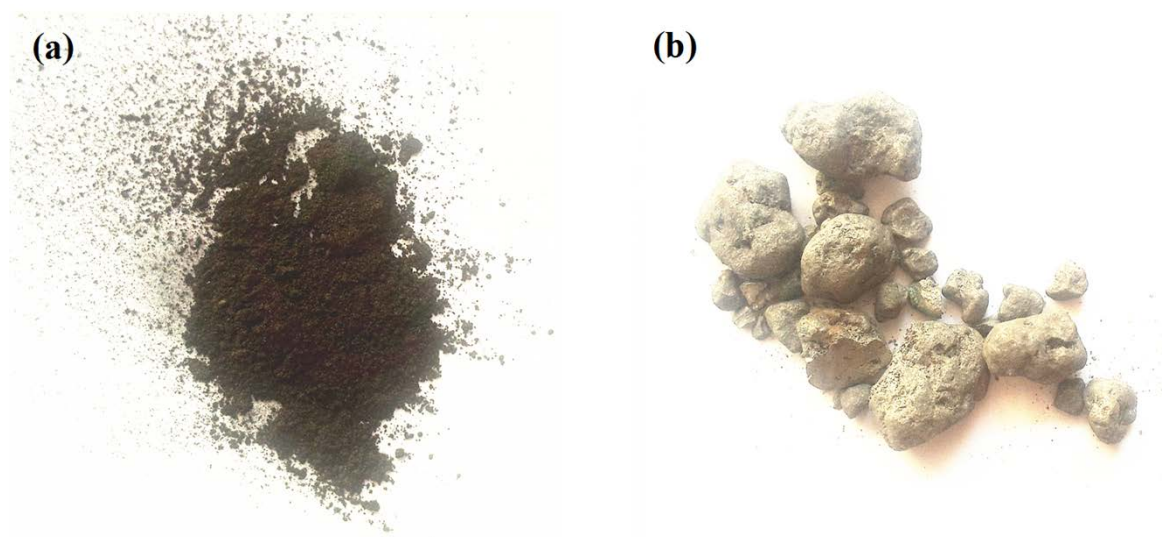


**Figure 1.** External view of raw materials with different ball milling durations: (a) 5 h and (b) 10 h.

The XRD image of the raw materials ball-milled for 5 and 10 h is shown in figure 2. After the raw material powders were ball-milled for 5 h, they were mainly composed of elemental Ti, Mo, and Ni. Thus, the raw materials did not undergo any reaction during the experimental procedure. After the powders were ball-milled for 10 h, the main components of the raw materials were Mo, (Ti,Mo)C, and NiTi. Therefore, the raw materials chemically reacted after the duration of ball milling was prolonged. Ball milling time affected the composition of raw materials. HEBM was conducted by using a rotating or vibrating machine to drive the grinding balls on the powders and achieve strong impact, grinding, and mixing influences; the powders were further broken down into small particles. Ball milling not only plays a significant role in mixing raw material powders but also in grinding them into small particle sizes and increasing the surface energy of particles. Particle size gradually decreases and temperature increases when milling time was extended to 10 h. As a result, Ti and C particles react and generate TiC, as expressed in the following chemical equation. In contrast to the peak of the standard PDF card, the actual peak was found at the right side. This phenomenon may be attributed to the incorporation of the Mo solution into TiC and the subsequent formation of (Ti,Mo)C. Mechanical

alloying occurs between the Ni and Ti components of the raw materials and an NiTi intermetallic compound forms through continuous ball milling, as expressed in the following equation:  $Ni + Ti \rightarrow NiTi$ . As a result, prolonged ball milling induces the raw materials to react with one another and produce (Ti,Mo)C. Therefore, the optimum ball milling time was 10 h.

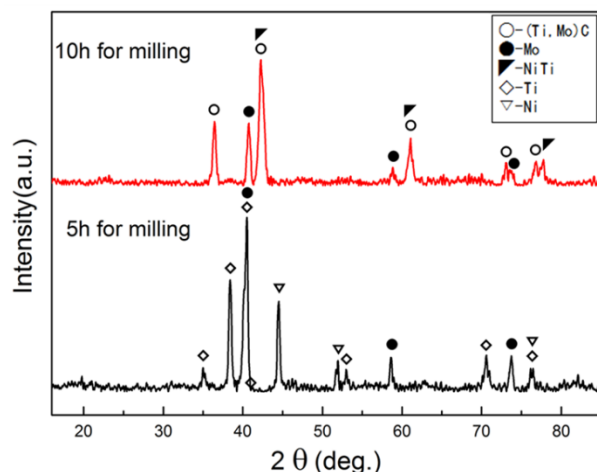


**Figure 2.** XRD patterns of raw materials ball-milled for 5 and 10 h.

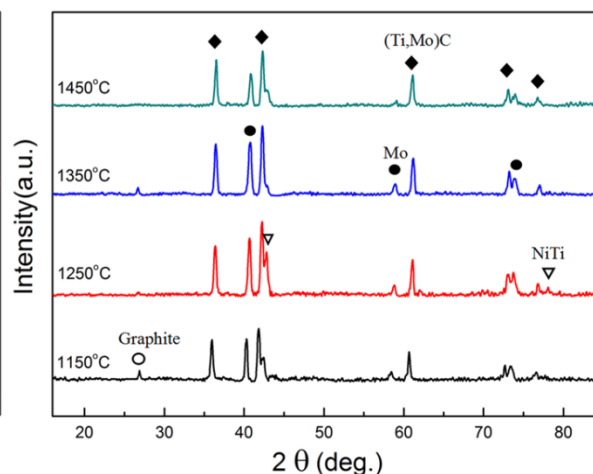


**Figure 3.** XRD patterns of the samples at different sintering temperatures ranging from 1150 °C–1450 °C.

### 3.2. XRD analysis of the samples at different sintering temperatures

The XRD patterns of the samples sintered at 1150 °C–1450 °C are shown in figure 3. At 1150 °C, the diffraction pattern reveals the diffraction peaks of (Ti,Mo)C, Mo, NiTi, and graphite. TiC was prepared. Compared with the position of the diffraction peak of the TiC standard, the position of the observed diffraction peak shifted. This phenomenon may be attributed to the incorporation of the Mo solution into the TiC and the formation of (Ti,Mo)C. As sintering temperature increases, the intensity of (Ti,Mo)C diffraction peak is enhanced to a certain extent. This result is possibly related to the growth of the grains. At high sintering temperatures, such as 1350 °C and 1450 °C, the intensity of the NiTi peak gradually weakened. This gradual weakening may be caused by a very high temperature, and some of the NiTi products were dissolved, and Ni, Ti were formed. Ti also reacts with C, and Ni is released.

### 3.3. Effects of sintering temperature on microstructure of composite TiC cermet

The composite TiC cermets produced by HEBM assisted SPS method possess high hardness. The sample sintered at 1150 °C has a high hardness value of 88.2 HRA. Figure 4 illustrates the SEM micrographs of the samples sintered at 1150 °C - 1450 °C. The microstructures of composite TiC cermet are composed of (Ti,Mo)C-Ni dark-gray phase, (Ti,Mo)C light-gray phase, and Mo white phase. Good wettability was observed among the different structures. The morphological characteristics of the sintered samples differed from the traditional core-ring structure; its center was the dark-gray phase surrounded by the light-gray phase and dispersed white phase. As sintering temperature increased, the grains gradually grew in size. For instance, the size of the dark-gray grains was approximately 0.5 μm (figure 4a). The average size of the particle increased to 3 μm when the sintering temperature was increased to 1450 °C (figure 4d). The grain size of two other structures also showed the same varying trend.

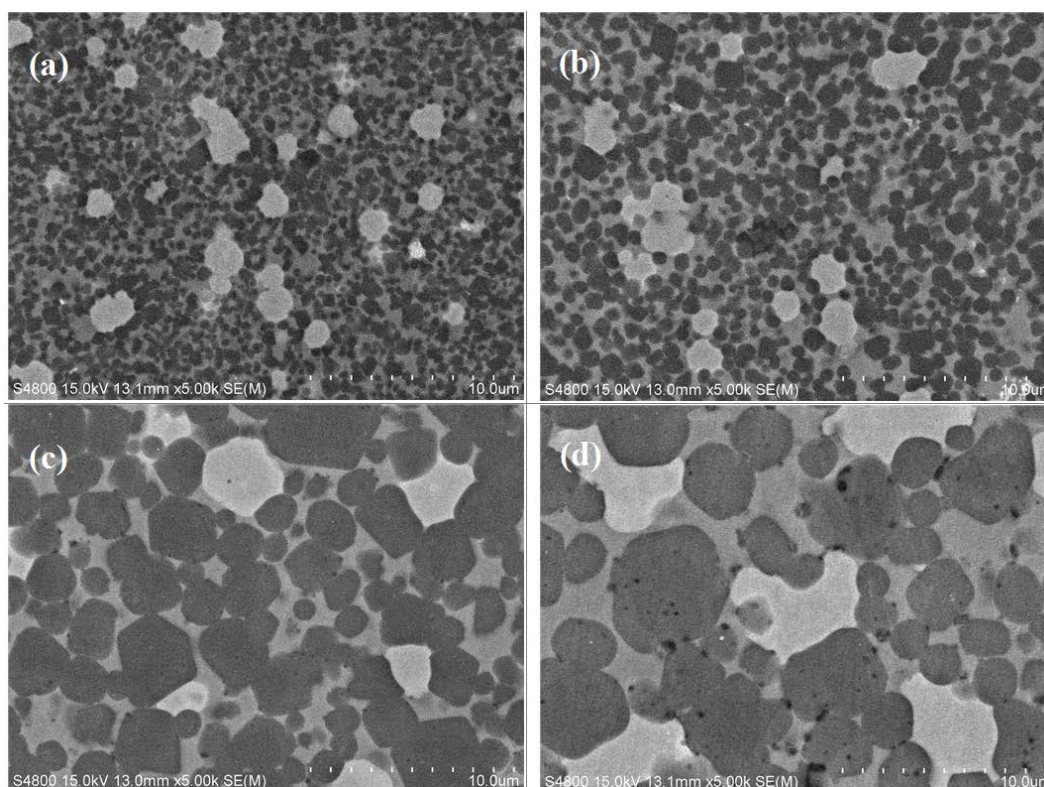


**Figure 4.** Microstructure of the samples at different sintering temperatures: (a) 1150 °C, (b) 1250 °C, (c) 1350 °C, and (d) 1450 °C.

#### 4. Conclusions

HEMB time significantly affects the raw materials. The raw materials can be ground into fine powders and produce a uniform mixture when they are ball-milled for 5 h. The raw materials can react become lumpy with a certain degree of hardness, and generate the (Ti,Mo)C when they are ball-milled for 10 h. The (Ti,Mo)C cermet with a high hardness value of 88.2 HRA was prepared at 1150 °C. The morphological characteristics of the sintered samples were different from those of the traditional core-ring structure. Dark-gray (Ti,Mo)C-Ni phase was found at the center surrounded by light-gray (Ti,Mo)C phase and large white dispersed Mo particles.

#### Acknowledgments

This work was supported by the National Natural Science Foundation of China (Grant No. 51464010), the Natural Science Foundation of Hainan Province (Grant No. 20165207), and the Middle-West part plan subject project of China (Grant No. ZXBJH-XK009).

#### References

- [1] R. Landfried, F. Kern and R. Gadow 2015 *Int. J. Refract. Met. Hard Mat.* **49** 334-8
- [2] P. Istomin, E. Istomina, A. Nadutkin and V. Grass 2016 *Int. J. Refract. Met. Hard Mat.* **57** 12-8
- [3] L. Tong and R.G. Reddy 2005 *Scripta Mater.* **52** 1253-8
- [4] L. Ding, D.P. Xiang, Y.L. Pan, T.M. Zhang and Z.Y. Wu 2016 *J. Alloys Compd.* **661** 136-40
- [5] D.W. Lee and B.K. Kim 2003 *Scripta Mater.* **48** 1513-8
- [6] M. Razavi, M.R. Rahimpour and A.H. Rajabi-Zamani 2007 *J. Alloys Compd.* **436** 142-45
- [7] Lai-Ma Luo, Xiao-Yue Tan, Hong-Yu Chen, Guang-Nan Luo, Xiao-Yong Zhu, Ji-Gui Cheng and Yu-Cheng Wu 2015 *Powder Technol.* **273** 8-12
- [8] Lixia Cheng, Zhipeng Xie and Guanwei Liu 2013 *J. Eur. Ceram. Soc.* **33** 2971-77